Journal of the Meteorological Society of Japan, Vol.79, No.6, pp.1139–1155, 2001

Simulation of Future Aerosol Distribution, Radiative Forcing, and Long-Range Transport in East Asia

By Toshihiko Takemura[1], Teruyuki Nakajima

Center for Climate System Research, University of Tokyo, Tokyo, Japan

Toru Nozawa

National Institute for Environmental Studies, Tsukuba, Japan

and

Kazuma Aoki

Institute of Low Temperature Science, Hokkaido University, Sapporo, Japan

(Manuscript received 11 April 2001, in revised form 31 July 2001)

Abstract

Distributions of aerosol concentrations, optical properties, and wet deposition fluxes are simulated for the next fifty years using an aerosol transport model coupled with an atmospheric general circulation model. Treated species are sulfur dioxide, and all the main tropospheric aerosols, i.e., carbonaceous (black and organic carbons), sulfate, soil dust, and sea salt. We especially pay attention to distributions of anthropogenic carbonaceous aerosols, sulfate aerosols, and sulfur dioxide. The simulation uses the Special Report on Emissions Scenarios (SRES) of the Intergovernmental Panel on Climate Change (IPCC) as the future emission scenarios of anthropogenic pollutants. Simulated results suggest that carbonaceous aerosols continue to increase over industrial and densely populated regions for the next five decades, whereas sulfate aerosols decrease around Europe and North America. The aerosol single scattering albedo in the future is, therefore, calculated to become small gradually in the mid- and high-latitudes of the Northern Hemisphere. Sulfate aerosols and sulfur wet deposition fluxes are, on the other hand, simulated to increase only over East Asia. Black carbon and sulfate aerosols around Japan in 2050 are simulated to be two or three times as large as those in 2000 with one of the SRES scenarios. Hence this suggests that pollutants originating from the East Asian continent can seriously affect the atmospheric quality in Japan in the next several decades.

1. Introduction

It is pointed out that anthropogenic and natural aerosols play the important roles in the climate change through two effects (e.g., IPCC 2001). One is the direct effect that aerosol particles scatter and absorb the solar and thermal radiation. The other is the indirect effect that they alter microphysical properties of cloud droplets acting as cloud condensation nuclei. Therefore, the radiative budget of the earth's atmosphere changes by increasing anthropogenic aerosols with industrialization. There are many past studies on the estimation of the global direct radiative forcing by anthropogenic sulfate and carbonaceous aerosols using climate models (e.g., Feichter et al. 1997;

Corresponding author: Teruyuki Nakajima, Center for Climate System Research, University of Tokyo, 4-6-1 Komaba, Meguro-ku, Tokyo 153-8904, Japan.
E-mail: teruyuki@ccsr.u-tokyo.ac.jp

1 Present affiliation: Research Institute for Applied Mechanics, Kyushu University

Penner et al. 1998; Kiehl et al. 2000), but the estimated forcings are largely different among the studies. This is mainly because the aerosol distribution is significantly inhomogeneous due to short lifetime in the atmosphere, various size distributions, and various chemical and optical properties of aerosol particles. Therefore it is important to develop a three-dimensional aerosol transport model which can treat all the main tropospheric aerosols of black carbon (BC), organic carbon (OC), sulfate, soil dust, and sea salt, by which the optical properties of the aerosol-laden atmosphere can be evaluated directly. Takemura et al. (2000) successfully compared the aerosol optical thickness as well as concentrations simulated by their aerosol transport model with global optical observations from space (e.g., Higurashi et al. 2000) and ground (Holben et al. 1998, 2001). The simulated single scattering albedo was also compared with the retrieval from the Aerosol Robotic Network (AERONET) radiance data (Dubovik and King 2000). Such validations will improve the accuracy of the radiative forcing evaluation from global climate models. It should be noted that their simulated direct radiative forcing of anthropogenic aerosols is $-0.2\,\mathrm{W\,m^{-2}}$ (Takemura et al. 2001), which is much smaller than the mean value summarized by the Third Assessment Report (TAR) of the Intergovernmental Panel on Climate Change (IPCC), i.e., $-0.5\,\mathrm{W\,m^{-2}}$ (IPCC 2001).

Anthropogenic aerosols and acid gases also have a harmful influence on the vegetation and human health. The wet deposition of sulfate and sulfuric gases, that is one of the main sources of acid rain as well as nitrate and nitric oxide (NO_x), has been indicated to lead to serious damage in Europe, East Asia, and the east part of North America (Langner and Rodhe 1991). The emission control of sulfur dioxide (SO_2) has been almost successful by the introduction of low-sulfur fuel and desulfurizers in industrially advanced countries. But the anthropogenic sulfur emission is predicted to continue increasing for the next several decades in developing countries (IPCC 2000). Therefore air pollution depends much on environmental policies of neighboring countries, because pollutants are transported not only inside the city but also from thousands of kilometers away, as suggested first in Northern Europe in the 1960's (Brossset and Akerstorm 1972). Moreover, a large amount of soot continues to be emitted mainly from diesel engines even in developed countries due to technical and economic difficulties to control its emission. The trace gases and aerosol particles emitted from anthropogenic biomass burnings, such as from plantations in tropical and subtropical regions, also cannot be ignored. It is said that global warming may increase the frequency and/or strength of extremely dry weather condition, which may further trigger large-scale biomass burnings such as the Indonesian forest fire event in 1997.

This study will simulated global distributions of anthropogenic and natural aerosols in the next five decades for understanding the regional changes in the chemical and rediative properties of the atmosphere around Japan, especially caused by transboundary transport of aerosols and their precursors. There have been several studies on the transportation and deposition of acid gases in East Asia (e.g., Regional Air Pollution Information and Simulation (RAINS)–Asia), but their main concerns were not oriented toward aerosol particles and their optical properties. For this simulation we adopt the Special Report on Emissions Scenarios (SRES) of the IPCC (IPCC 2000), which is the newest data set on emissions of anthropogenic trace gases during the 21st century instead of an old data set so-called the IS92 scenario (IPCC 1992). The SRES scenarios include main driving forces of demographic, technological, and economic developments, and they are divided into four qualitative storylines, i.e., A1, A2, B1, and B2. The A1 storyline describes a future world of very rapid economic growth, increase of population, and introduction of new or more efficient technologies with a substantial reduction in regional differences. The A2 storyline represents a very heterogeneous world assuming the importance of local identities for economic and social activities. On the other hand, the B1 storyline is oriented toward global environmental protection with a well-balanced economic structure, and the B2 is similar to the B1 but with policies in regional levels. The each storyline has an illustrative scenario. In Section 2 we will describe the method of making grid data of emitted pollutants according to the SRES scenarios for use in the climate model. The provided data by the SRES are divided only into several regions of the world, so that we have to increase the spatial resolution of the emission data for better representation of the regional characteristics for the detailed regional study. Moreover, the emission data for carbonaceous aerosols is not included in the scenario, so that we prepare it referring to the sce-

nario data on budgets of carbon dioxide (CO_2). In Section 3 the simulated future global aerosol distributions, deposition fluxes, and optical properties will be considered. In Asia except Japan, the emission flux of SO_2 tends to increase rapidly since 1970 as indicated by Kato and Akimoto (1992) and Lefohn et al. (1999), and it is also predicted by the SRES scenarios to continue increasing for the 21st century including other anthropogenic pollutants. We will, therefore, particularly focus on the present and future long-range transport from the East Asian continent to Japan in Section 4. The pH in a raindrop mainly depends on concentrations of acid gases, such as SO_2 and NO_x, and neutralizers. Samplings of acid rain by the Ministry of the Environment of Japan since 1983 have indicated low pH values below 5.6 over the most parts of Japan. Moreover, lower pH values have been measured in the west part of Japan than the east part. These observations suggest the serious influence of long-range transport of pollutants from the East Asian continent to Japan. In this study we will discuss these points with the simulated results of the present and future aerosol concentrations, and sulfur wet deposition fluxes in Japan affected by polluted air from the continent.

2. Model description and emission scenario

The three-dimensional aerosol transport model used in this study can simultaneously treat main trospospheric aerosols of sulfate, carbonaceous (BC and OC), soil dust, and sea salt. The detailed aerosol transport processes of this model are described in Takemura et al. (2000), and optical properties and revised transport processes are shown in Takemura et al. (2001). The present model is coupled to the dynamical and physical processes of the atmospheric general circulation model (AGCM) of the Center for Climate System Research (CCSR), University of Tokyo/National Institute for Environmental Studies (NIES), Japan (Numaguti et al. 1995). The model horizontal resolution of the triangular truncation is set at T42 (approximately 2.8° by 2.8° in longitude and latitude), and the vertical resolution is 11 layers which are finer for lower altitudes. The initial conditions of dynamical and physical parameters, and the boundary conditions of sea surface temperature and sea ice, are obtained from the simulation by the CCSR/NIES coupled ocean-atmosphere general circulation model for corresponding times and scenarios (Nozawa et al. 2001). The aerosol transport processes include the emission, advection, diffusion, sulfur chemistry, and deposition. Sulfur species treated explicitly in this model are dimethylsulfide (DMS), SO_2, and sulfate. The deposition process is divided into four mechanisms, i.e., sub-cloud scavenging, in-cloud scavenging, dry deposition, and gravitational settling. The two-stream discrete ordinate/adding method is adopted for radiative process calculations with eight bands in the solar spectral region and ten in the thermal spectral region (Nakajima et al. 2000). The size distributions, optical parameters, and hygroscopic growth are assumed to be different among aerosol species (Takemura et al. 2001).

The SRES anthropogenic SO_2 emission flux has been prepared in four regions of the world (OECD; Eastern Europe and Former Soviet Union; Asia; Africa, Middle East, and Latin America) for each scenario and every decade from 1990 to 2100. Then the gridded emission pattern within each region follows the Global Emissions Inventory Activities (GEIA) database for SO_2 (Benkovitz et al. 1996). The future emission scenario of BC has to be provided for fossil fuel, biomass burning, and biomass fuel origins for the simulation, but it is not included in the SRES data sets. Therefore a BC emission inventory has been made from the CO_2 emission of the SRES scenarios, and scaled and gridded using the GEIA database for fossil fuel and biomass burning (Cooke and Wilson 1996) and our database by Takemura et al. (2000) for biomass fuel. The GEIA data on the BC emission is within a factor of 2 in comparison with measurements. These gridded emission scenarios are prepared as annual mean data except for biomass burning sources for which monthly mean data are prepared. The OC emission is derived from the BC emission assuming a ratio of OC to BC for each source according to the method proposed by Takemura et al. (2000). The SO_2 emission from volcanoes, and the carbonaceous aerosol emission from agricultural wastes and vegetation are provided as constant in times and scenarios. Soil dust, sea salt, and DMS emissions are calculated using meteorological parameters within the model (Takemura et al. 2000). The sulfur chemistry is calculated with the monthly mean three-dimensional oxide fields of OH, H_2O_2, and ozone prescribed from the CCSR chemistry transport model (Sudo and Takahashi 2001) with the future changes of their global mean concentrations simulated by the other chemical transport model among the SRES scenarios (Collins et al. 1997).

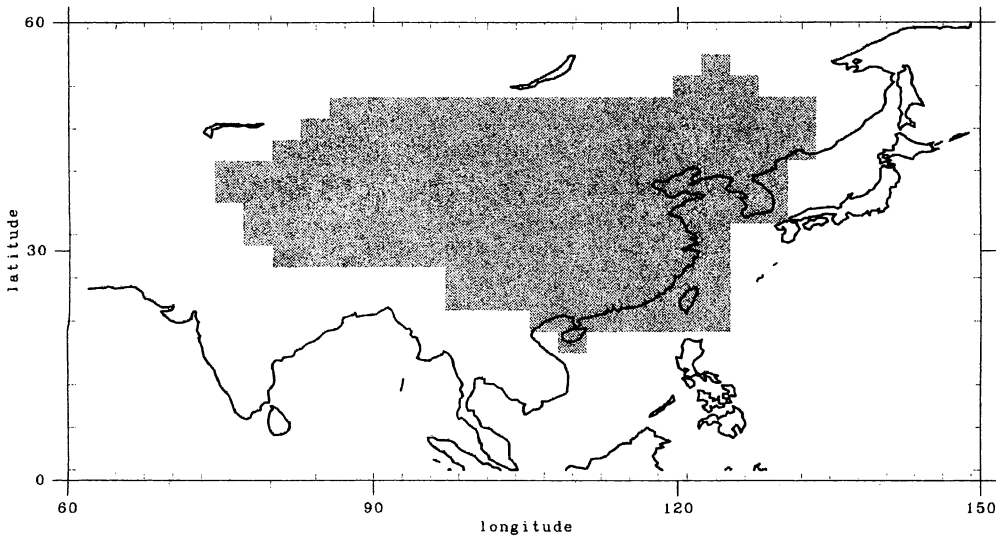

Fig. 1. Definition of the East Asian continent in this study.

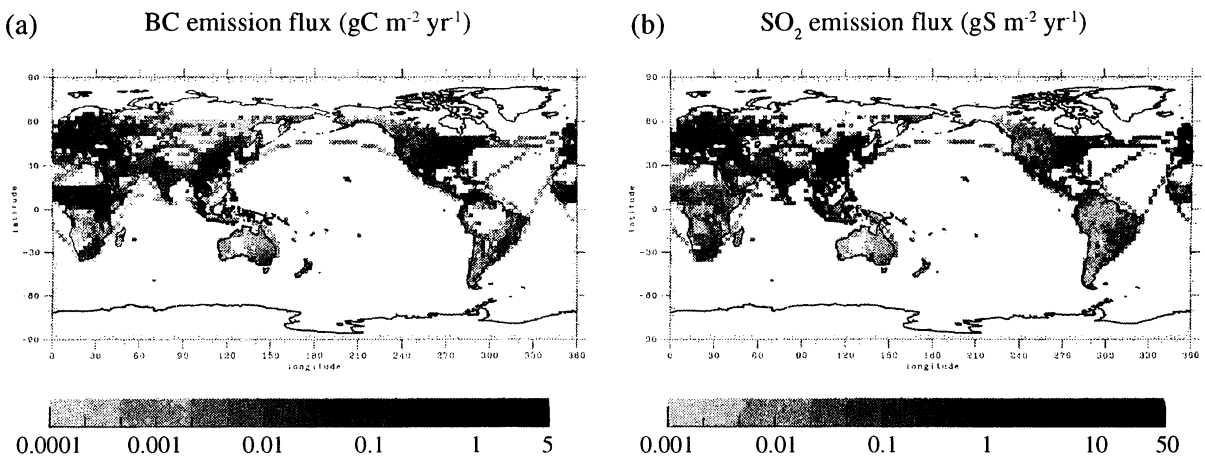

Fig. 2. Global distributions of the annual (a) BC and (b) SO_2 emissions fluxes in 2000 from anthropogenic sources.

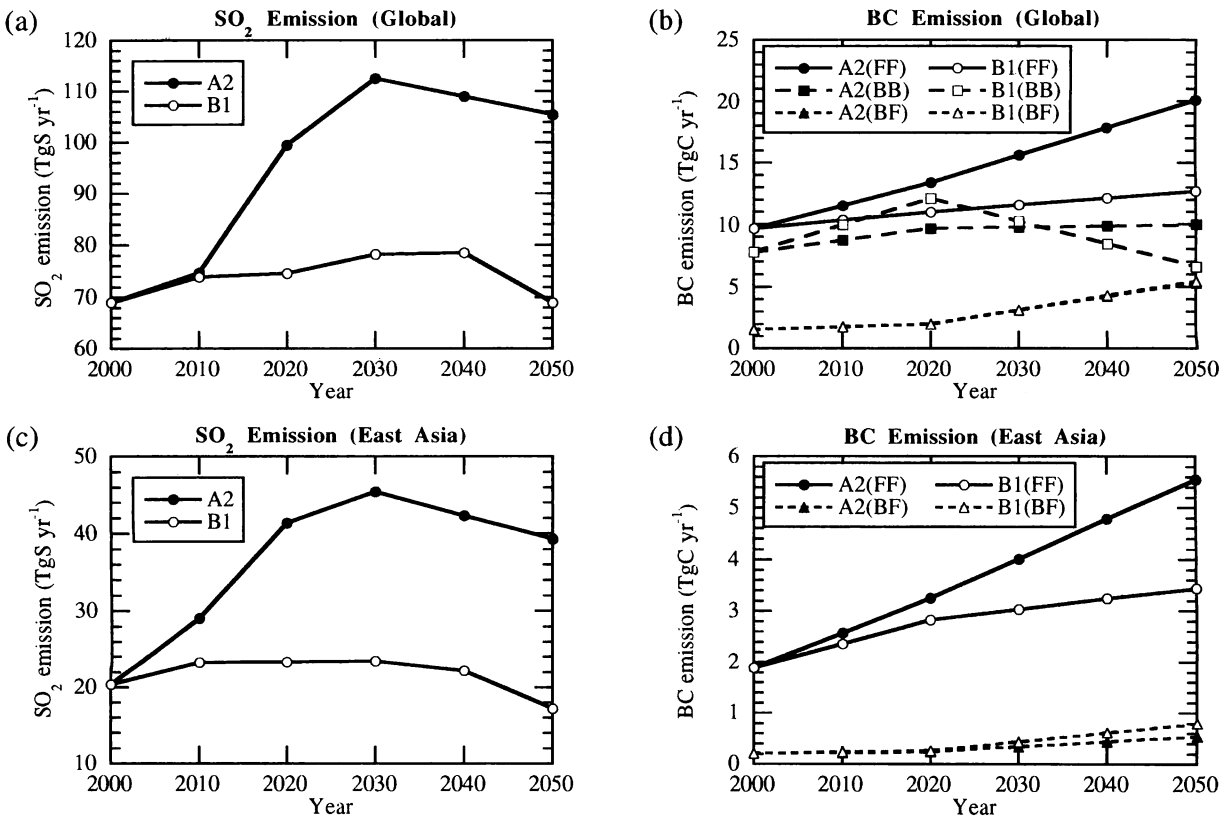

Fig. 3. Time series of future global emissions of (a) SO_2 ($TgS\,yr^{-1}$) and (b) black carbon ($TgC\,yr^{-1}$) and East Asian emissions of (c) SO_2 ($TgS\,yr^{-1}$) and (d) black carbon ($TgC\,yr^{-1}$) from 2000 to 2050 based on the SRES scenarios. 'FF', 'BB', and 'BF' denote fossil fuel, biomass burning, and biomass fuel origins, respectively.

The present and future concentrations of CO_2, CH_4, and N_2O also follow the SRES scenarios. Thirteen species of halocarbons are also considered, but their temporal variations are common to all scenarios. The simulations are carried out every decade from 2000 to 2050 for the A2 and B1 scenarios in this study. These two scenarios are selected because emission fluxes of pollutants in the A2 and B1 are almost maximum and minimum, respectively, among the four scenarios. To evaluate the long-range transport from the East Asian continent to Japan, another simulation is performed with masking emissions of all aerosol species and SO_2 from the continent. In this study the East Asian continent is defined as shown in Fig. 1. Figure 2 shows the global distributions of the annual BC and SO_2 emission fluxes in 2000 from anthropogenic sources, and Fig. 3 shows the time series of the SO_2 and BC emissions of the global total and of the East Asian continent alone. The SO_2 emission of the A2 scenario reaches the maximum in 2030 and then decreases both for the global total and East Asia, though that of the old scenario, i.e., IS92a, continues to increase till 2050 when the emission flux of the global total becomes $153\,TgS\,yr^{-1}$. The difference in the A2 emission fluxes between 2000 and 2030 in the East Asian continent is about $25\,TgS\,yr^{-1}$, which contributes to more than half of the increasing rate of the global emission. The SO_2 emission flux in East Asia accounts for 40% of that of the global total in 2030 in the A2 scenario. In the B1 scenario, on the other hand, it is nearly constant from 2000 to 2050. The SO_2 emission from Japan is projected

to be two others smaller than that from the East Asian continent for both scenarios. The BC emission originating from fossil and biomass fuels continues to increase globally till 2050 in both the A2 and B1. In the East Asian continent BC is predicted to be emitted three times in 2050 as much as in the present day in the A2 scenario. The BC emission flux from fossil fuel consumption in Japan is 0.30 TgC yr^{-1} in 2000, and 0.42 TgC yr^{-1} for the A2 and 0.27 TgC yr^{-1} for the B1 in 2050, respectively. The technologies for removing particle matters are being introduced in developed countries, such as Japan, but not considered for the future BC emission in this study which refers to the gaseous emission of CO_2, so that the estimated BC emission may be overestimated. Differences in the aerosol optical thickness in the present day between the simulation and observations are less than 30% at the representative sites of the AERONET (Takemura et al. 2001) and the comparisons in Japan are also carried out in Section 4.

3. Future global characteristics of aerosol distributions and their optical properties

Figure 4 shows the simulated present and future distributions of carbonaceous and sulfate aerosol concentrations at the lowest atmospheric layer, whose sigma level is 0.995. According to the simulation based on the A2 scenario, carbonaceous aerosols in 2050 increase around the densely populated regions such as Asia, Europe, and North America in comparison with the present day situation. The global annual mean burden of atmospheric carbonaceous aerosols by the A2 simulation in 2050 is calculated to be 1.6 times as large as that in 2000. The increasing rate of carbonaceous aerosols is especially large over East and South Asia, and the annual mean burden of the A2 simulation in 2050 is 2.5 times as large as that in 2000 in the region defined by Fig. 1. In 2050 along the B1 scenario. carbonaceous aerosol concentrations are simulated to be close to those in 2000 over Europe and North America, whereas they increase over East and South Asia though this scenario has the smallest emission fluxes of pollutants in the SRES. It is also predicted that carbonaceous aerosols emitted from forest fires become prominent around Southeast Asia for the next fifty years in both scenarios.

The mass ratio of sulfate aerosols in East Asia to the global total amount is calculated to be larger in 2050 than in 2000 for both scenarios. East Asia, however, has almost the same sulfate concentrations between 2000 and 2050 in the B1 simulation. It is projected to introduce low-sulfur fuel and desulfurizers gradually in a few decades even in developing countries according to the B1 scenario, so that the generating rate of sulfate aerosols is simulated to stop increasing until 2050. On the other hand, in the A2 simulation, the sulfate aerosol concentration in 2050 in more than twice as large as in 2000 around East Asia. Europe and North America have much lower sulfate concentrations in 2050 than in 2000 for both simulations. The global total annual mean burden of sulfate aerosols is calculated to be 0.442 TgS in 2000; 0.709 and 0.526 TgS in 2050 of the A2 and B1 simulations, respectively.

The simulation of the sulfur wet deposition flux is important in order to discuss acid rain and long-range transport predictions. Figure 5 shows that the wet deposition is calculated to be as large as 0.5 gS m^{-2} yr^{-1} over most parts of Europe and Northeast U.S. in 2000, which is close to the simulation of Langner and Rodhe (1991) based on emission database in 1980's. The simulation over East Asia is, on the other hand, more than 1.0 gS m^{-2} yr^{-1}, which is about twice as large as that of Langner and Rodhe (1991). This difference reflects the recent rapid economic growth in East Asia taken into account in the new scenario. The simulated result suggests that East Asia has already become the most polluted region of the world. Difference in atmospheric pollution between East Asia and other industrial regions is simulated to extend in 2050. The sulfur wet deposition flux by the A2 simulation in 2050 is 1.8 times as large as that in 2000 in East Asia. It is possible that the problem of acid rain in this region becomes more serious in the next several decades. In the simulation based on the B1 scenario, the sulfur wet deposition in 2050 is almost the same as that in 2000 in East Asia, though it decreases substantially in Europe and North America. Therefore it is unlikely that the acid rain phenomenon in East Asia is improved in the next several decades considering the convincing future social developments in this region.

Figure 6 shows the aerosol optical thickness and single scattering albedo in a mixed polydispersion of main tropospheric aerosol species of carbonaceous, sulfate, soil dust, and sea salt simulated along the SRES scenarios. The optical thickness is predicted to become much larger in 2050 around

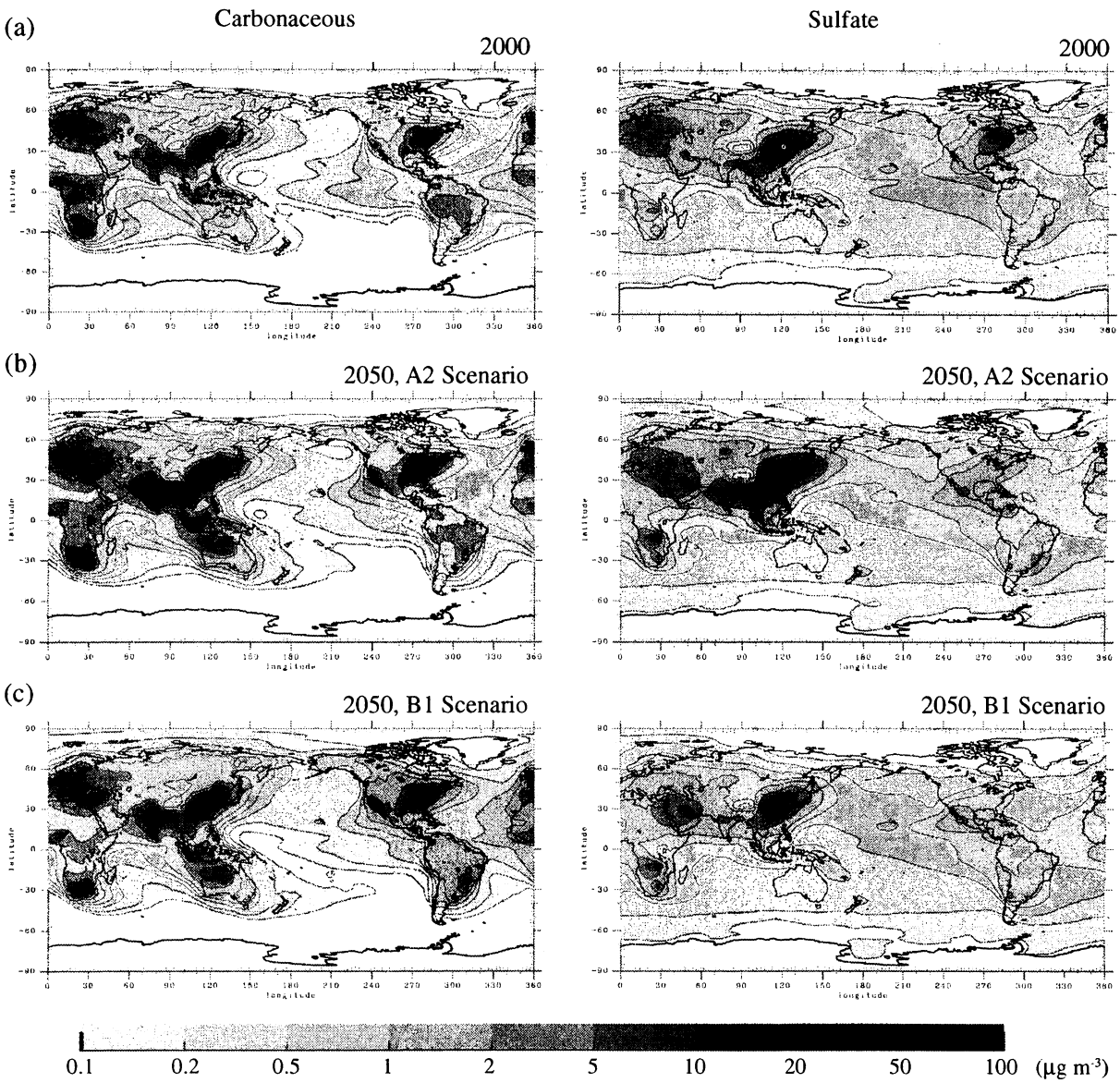

Fig. 4. Annual mean distributions of the simulated carbonaceous (left) and sulfate (right) aerosol concentrations in $\mu g\,m^{-3}$ at the lowest model layer (the sigma level is 0.995) in (a) 2000, (b) 2050 of the A2 scenario, and (c) 2050 of the B1 scenario.

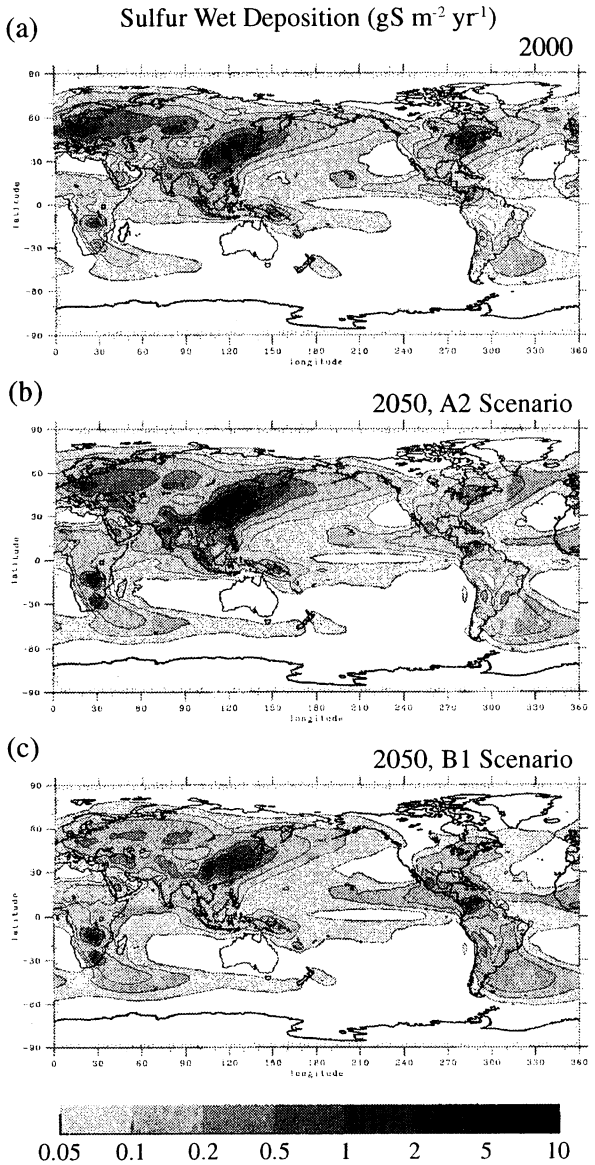

Fig. 5. Annual mean distributions of the simulated wet deposition flux of sulfur species including SO_2 and sulfate aerosols in $gS\,m^{-2}\,yr^{-1}$ in (a) 2000, (b) 2050 of the A2 scenario, and (c) 2050 of the B1 scenario.

East Asia than in 2000 for the A2 scenario. This large amount of pollutants is also transported to the Northwest Pacific. The simulated annual mean value of the maximum optical thickness in East Asia is less than 0.7 in 2000, while it becomes more than 1.5 in 2050 of the A2 simulation. In the simulation based on the B1 scenario, the optical thickness in 2050 is almost the same as that in 2000 around East Asia. The most significant characteristic of the simulated single scattering albedo is that it is projected to become small for the next several decades in the mid- and high-latitudes of the Northern Hemisphere. This is because the ratio of column burden of anthropogenic BC to sulfate aerosols is predicted to become large, so that absorption of the solar radiation due to BC will become more dominant.

Table 1 summarizes the direct radiative forcing of carbonaceous and sulfate aerosols. In this table, the clear-sky is defined as the cloudless atmospheric condition and the whole-sky means the atmospheric condition with clouds. The difference in the radiative forcings between clear-sky and whole-sky conditions occurs because cloud layers enhance the radiative absorption of aerosol particles, such as BC, due to multiple scattering of the solar radiation, and also because they attenuate the incident solar radiation falling onto aerosol particles, as discussed in detail by Takemura et al. (2001). The global annual mean value of the simulated sulfate radiative forcing related with fossil fuel consumption in 2000 is $-0.30\,W\,m^{-2}$, and it increases almost twice in 2050 in the A2 simulation. It is also slightly larger in 2050 than in 2000 in the B1 simulation though there is little difference in the global emission of SO_2 between 2000 and 2050 (Fig. 3a). This is because the column burden of sulfate aerosols is slightly larger in 2050 due to unstable atmosphere affected by the global warming. The BC radiative forcing is also calculated to become larger in 2050 than in 2000 for both scenarios. Hence it is found that BC offsets the cooling effect of sulfate aerosols profoundly in 2050 for the whole-sky condition in the A2 simulation. The direct radiative forcing of OC from fossil fuel consumption is simulated to be smaller than that of BC on the opposite sign, whereas the forcing value of carbonaceous aerosols from biomass burning is close to zero or slightly negative due to the large mass ratio of OC to BC, which is in agreement with the estimation based on the observation (Hobbs et al. 1997).

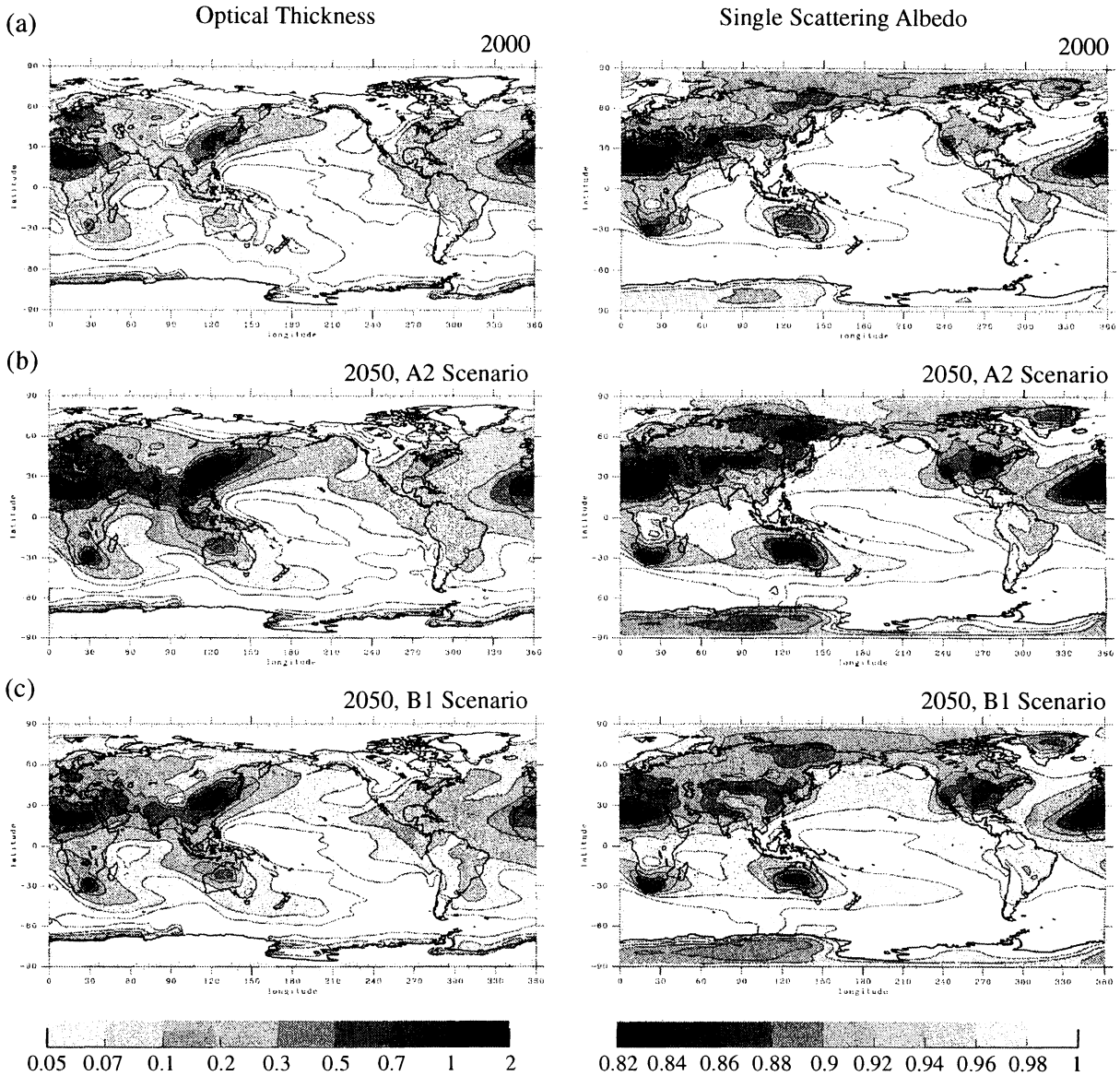

Fig. 6. Annual mean distributions of the simulated aerosol optical thickness (left) and single scattering albedo (right) for a mixed polydispersion of all aerosol species, i.e., carbonaceous (black and organic carbons), sulfate, soil dust, and sea salt in (a) 2000, (b) 2050 of the A2 scenario, and (c) 2050 of the B1 scenario.

Table 1. Global annual mean direct radiative forcings of carbonaceous and sulfate aerosols at the tropopause for whole- and clear-sky conditions in 2000 and 2050 of the A2 and B1 scenarios, calculated by the present model in $W\,m^{-2}$. The forcings of aerosols from fossil fuel (FF) and/or biomass burning (BB) sources are also shown separately.

	Whole-sky			Clear-sky		
Year	2000	2050 (A2)	2050 (B1)	2000	2050 (A2)	2050 (B1)
Carbonaceous	+0.04	+0.15	+0.10	-0.40	-0.61	-0.45
OC	-0.29	-0.46	-0.32	-0.59	-0.96	-0.70
FF	-0.06	-0.13	-0.10	-0.14	-0.29	-0.20
BB	-0.19	-0.22	-0.13	-0.36	-0.44	-0.28
BC	+0.33	+0.61	+0.42	+0.19	+0.35	+0.25
FF	+0.17	+0.40	+0.27	+0.12	+0.22	+0.18
BB	+0.13	+0.14	+0.11	+0.07	+0.06	+0.06
Sulfate	-0.38	-0.63	-0.46	-0.80	-1.26	-0.91
FF	-0.30	-0.54	-0.38	-0.63	-1.09	-0.74

OC = Organic carbon, BC = Black carbon.

4. Long-range transport of pollutants from the East Asian continent to Japan

It is predicted that emissions of various anthropogenic pollutants will greatly increase due to the rapid economic and industrial growths in East Asia except Japan in the next several decades as mentioned in Section 2. Therefore it is possible that a serious atmospheric pollution will be caused by long-range transport from the East Asian continent to Japan, where strong antipollution measures have been already promoted. Here we study simulated results of the present and future aerosol concentrations, optical thickness, and sulfur wet deposition in Japan affected by emissions from the continent.

To secure the accuracy of the projectional simulation, the performance of the present model has been validated using aerosol optical measurements in Japan. Figure 7 shows comparisons of the simulated aerosol opitical thickness and Ångström exponent in 2000 with retrieved values from the PREDE sky radiometer POM-01, which is a sun/sky photometer manufactured by PREDE Co. Ltd., at three sites available of the SKYNET in Japan. It should be noted that observation years are not necessarily the same as the simulation year, which may introduce an additional difference between observed and simulated results. The optical thickness and Ångström exponent in Niigata and Tsukuba, are in good agreement between the simulation and observations. The optical thickness in Niigata takes its maximum in spring due to heavy long-range transport of anthropogenic pollutants and Asian dust from the continent. It is also suggested from the model results that the large optical thickness and Ångström exponent in summertime are caused by dominance of sulfate aerosols because of active chemical reactions and hygroscopic growth in this season. Carbonaceous aerosols are a main contributor to the total optical thickness as well as sulfate aerosols, and their optical thickness is simulated to be about 0.1 through the year in the present. Tsukuba also has the maximum optical thickness in spring both for the simulation and observation. It is found that the decrease in the optical thickness in the rainy season of July is simulated as well. The contribution ratios to the total optical thickness are almost constant through the year for both carbonaceous and sulfate aerosols. The simulated optical thickness in Sapporo is, on the other hand, overestimated from summer to the end of the

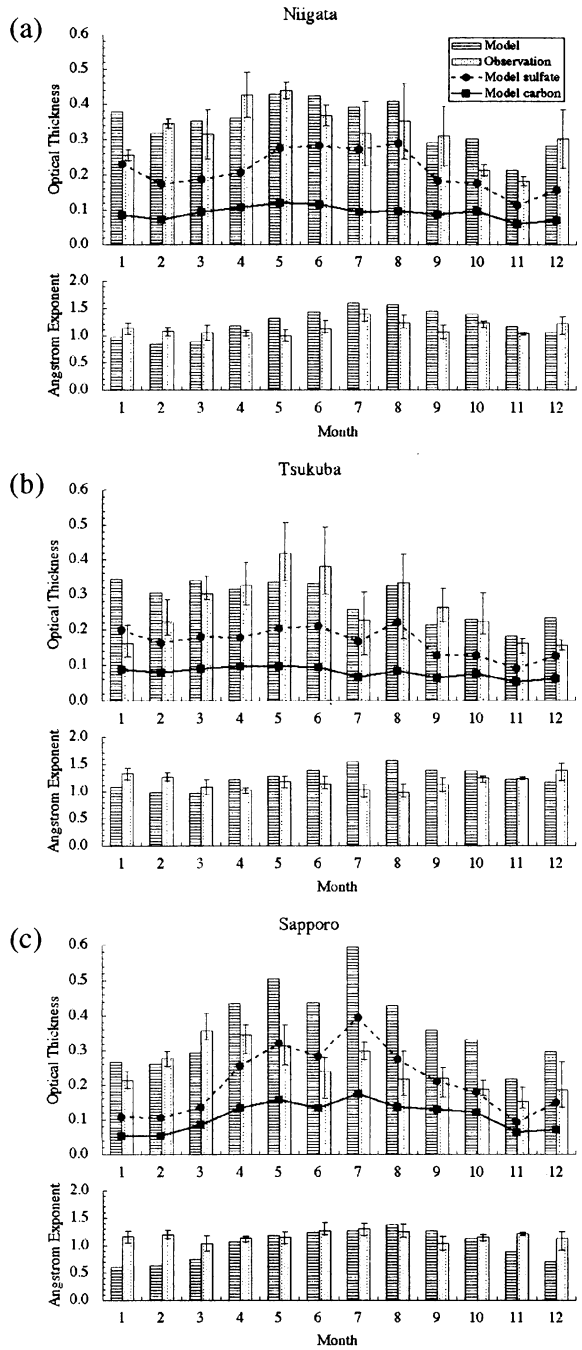

year. This overestimation can be explained by the slightly difference in the wind direction between the AGCM and the real field around 43°N, so that long-range transport from China and Korea is overestimated by the model.

Figure 8 shows simulated monthly mean values of the BC concentration with its contribution originating from the East Asian continent defined in Fig. 1 in 2000 and 2050. The annual mean value are also shown in Table 2. The target regions are the northern Nansei Islands (Fig. 8a), northern Ogasawara Islands (Fig. 8b), southern coast of Kanto district (Fig. 8c), and southwestern Hokkaido (Fig. 8d). The northwesterns wind is prominent in winter around Japan, so that the outflow of pollutants from big cities of China seriously affects southwestern regions of Japan, such as the Nansei Islands and the Ogasawara Islands (Figs. 8a and 8b). On the other hand, the BC concentration and its contribution from the continent are low in summer in these regions due to the domination of the North Pacific Anticyclone. The Nansei Islands and the Ogasawara Islands have much higher BC concentration in 2050 for both scenarios than in 2000 through the year. The contribution of the continent around the Kanto Plain, which is the most densely populated region in Japan, is simulated to be less than those in the above two regions (Fig. 8c and Table 2). It is thought that the contribution ratio from the continent is still less within the big cities such as Tokyo. The BC concentration is calculated to be almost unchanged around the Kanto Plain for the five decades in the B1 simulation because the BC emission from Japan is predicted to be nearly constant. The BC concentration at the southwestern Hokkaido is calculated to be the largest in summer (Fig. 8d) though it should be noticed that the simulated optical thickness is larger

Fig. 7. Comparisons of monthly mean values of simulated and observed aerosol optical thickness at 0.55 μm and Ångström exponents at (a) Niigata (139.00E, 37.92N), (b) Tsukuba (140.13E, 36.05N), and (c) Sapporo (141.34E, 43.08N). Simulated optical thickness for only sulfate and carbonaceous aerosols are also shown. Obseravtion periods are from January 1995 to December 1995 and from July 1996 to June 1997 at Niigata, from May 1996 to April 2000 at Tsukuba, and from October 1997 to September 2000 at Sapporo.

than the observation in the latter half of the year. The contribution of the continent is maximum in March and April 2000, which is in correspondence with the observed long-range transport of Asian dust to Japan and the North Pacific.

Seasonal variabilities of the simulated sulfate contribution of the continent is similar to those of BC as shown in Fig. 9, but the ratio is much higher for sulfate aerosols in all the target regions in Japan. The annual mean contribution of the continent is calculated as large as 82% for sulfate aerosols in 2000 around the southwestern Hokkaido, whereas 30% for BC (Table 2). This contribution difference is mainly caused by the recent rapid increase in the anthropogenic SO_2 emission in the East Asian continent. The ratio is predicted to be further higher *in 2050* with the A2 scenario, and sulfate concentrations are more than twice as large as those in 2000 in each region. This simulated result suggests that the atmospheric quality in Japan can become worse due to sulfur species in the future several decades because of the heavy anthropogenic emission from neighboring countries, though the pollution in Japan was caused by local emissions several decades ago. Figure 10 shows the simulated wet deposition flux of sulfur species including SO_2 and sulfate aerosols every decade in four regions. It is projected to change little for the next fifty years in the B1 simulation, while it increases twice in 2030 as large as in 2000 and keeps the high value till 2050 in the A2 simulation. The contribution of the continent is also above 80% in the next fifty years in the A2 simulation. The GEIA database on SO_2, which is used for making gridded data, is a little rough for the regional study, so that the contribution ratio of the continent for the sulfur wet deposition may be overestimated. The wide-area pollution such as destruction of forests due to acid rain has become serious in Europe and North America since 1970's, and the simulation suggests that it will occur not only in the East Asian continent but also in Japan in a next few decades if emissions of anthropogenic pollutants continue to increase as projected by the A2 scenario.

Simulated monthly changes between the optical thickness and its contribution of the continent almost synchronize temporarily in all the target regions (Fig. 11). This suggests that variabilities of

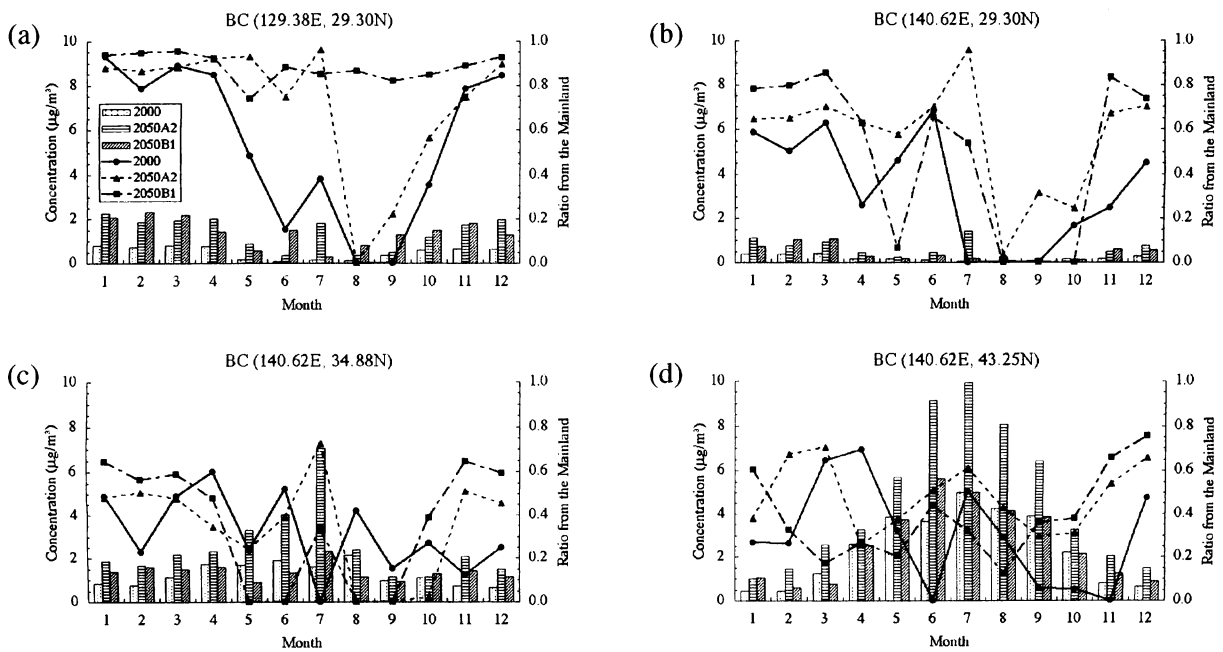

Fig. 8. Monthly mean values of the simulated black carbon concentration in $\mu g\,m^{-3}$ at the lowest model layer (the sigma level is 0.995) (column with left scale) and its contribution ratio originating from the East Asian continent (line with right scale) at four grid points in Japan in 2000 and 2050 of the A2 and B1 scenarios.

Table 2. Annual mean aerosol concentrations and optical thickness with ratios of pollutants from the East Asian continent in 2000 and 2050 of the A2 and B1 scenarios at four grid points in Japan simulated by the present model.

	Black carbon		Sulfate		Total	
	Concentration ($\mu g\ m^{-3}$)	Ratio (%)	Concentration ($\mu g\ m^{-3}$)	Ratio (%)	Optical thickness	Ratio (%)
129.38E, 29.30N						
2000	0.49	54	5.58	70	0.23	55
2050 (A2)	1.41	72	11.25	83	0.45	72
2050 (B1)	1.41	88	7.51	84	0.35	60
140.62E, 29.30N						
2000	0.20	33	2.06	53	0.13	36
2050 (A2)	0.60	57	4.75	77	0.24	57
2050 (B1)	0.43	49	2.38	54	0.16	45
140.62E, 34.88N						
2000	1.27	32	5.23	65	0.25	46
2050 (A2)	2.56	35	11.31	79	0.47	62
2050 (B1)	1.38	35	4.36	70	0.28	54
140.62E, 43.25N						
2000	2.42	30	6.46	82	0.37	59
2050 (A2)	4.54	48	13.21	92	0.66	74
2050 (B1)	2.63	38	4.18	84	0.36	60

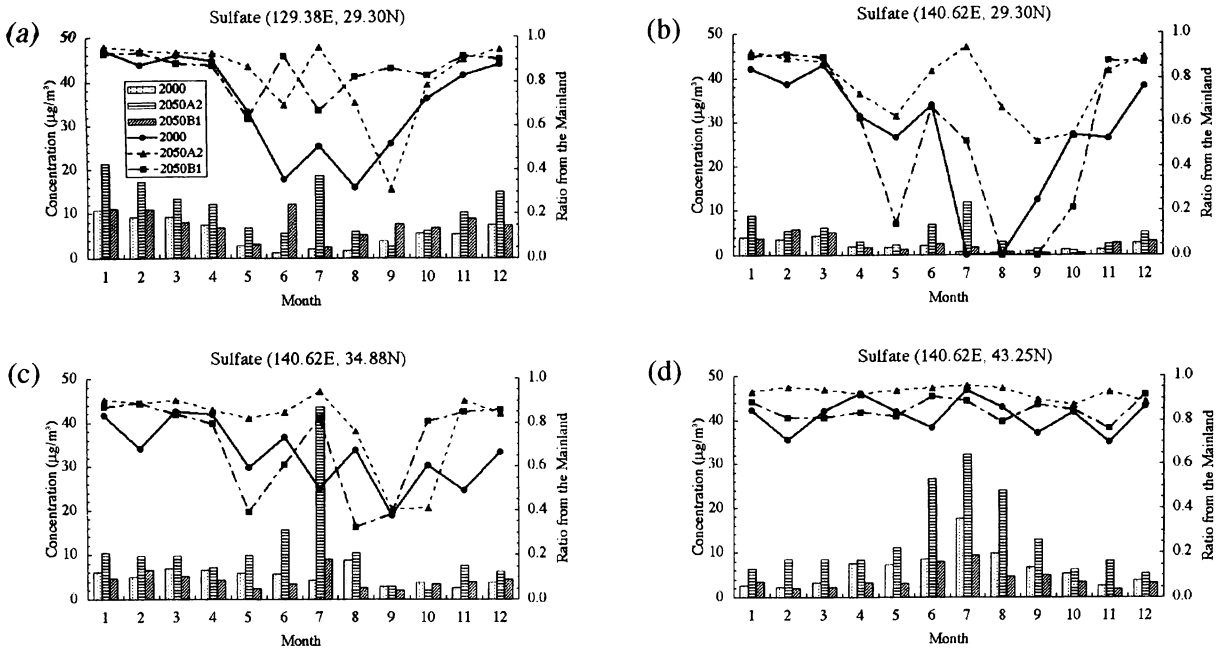

Fig. 9. Same as Fig. 8 but for the sulfate aerosol concentration.

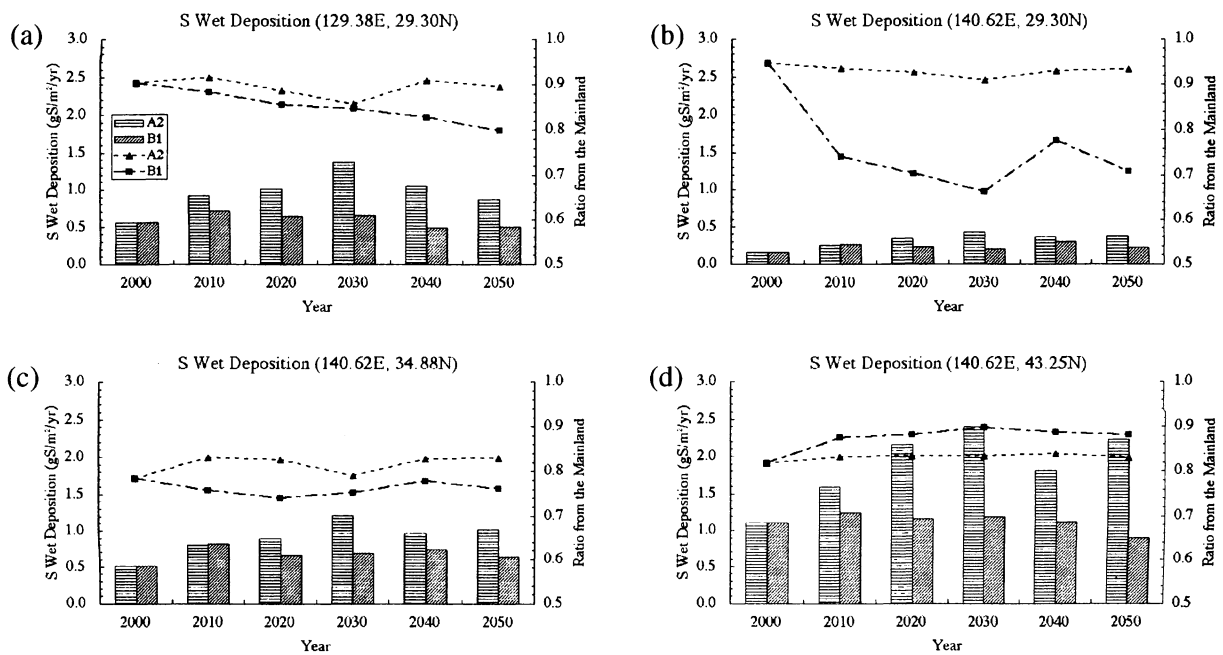

Fig. 10. Annual mean values of the simulated wet deposition flux of sulfur species including SO_2 and sulfate aerosols in $gS\,m^{-2}\,yr^{-1}$ (column with left scale) and its contribution ratio originating from the East Asian continent (line with right scale) at four grid points in Japan from 2000 to 2050 for the A2 and B1 scenarios.

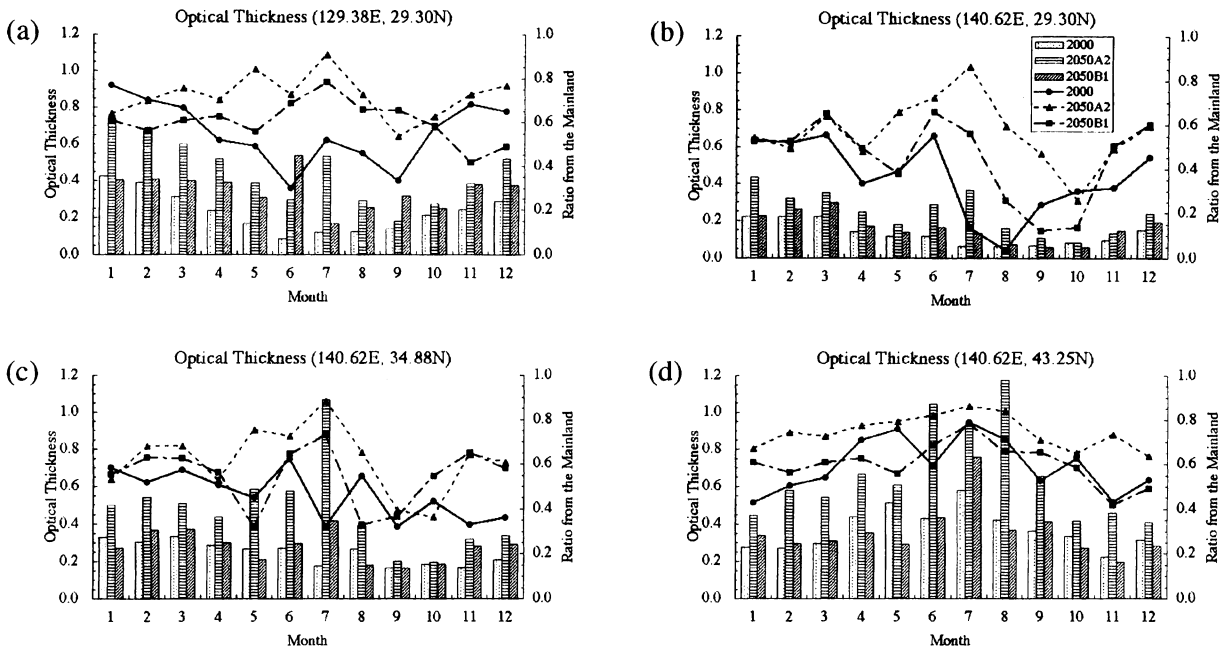

Fig. 11. Same as Fig. 8 but for the aerosol optical thickness.

long-range transport of pollutants affect the column burden more directly than the surface concentration. In general, the peak of the aerosol concentration appears at a height of a few kilometers at remote regions from emission sources (Takemura et al. 2000). The optical thickness in 2050 is predicted to be about twice as large as in 2000 in the A2 simulation, so that it is apprehensive that anthropogenic aerosols originating from the East Asian continent will have serious impacts on the climate and the atmospheric chemical environment through the aerosol direct and indirect effects even in Japan and the North Pacific.

5. Conclusions

The gridded database of the present and future emissions for anthropogenic BC and SO_2 were made along the SRES scenarios, and then global distributions of aerosol concentrations, aerosol optical properties, and sulfur wet deposition were predicted for the next fifty years with our aerosol transport model coupled with the CCSR/NIES AGCM. The BC surface concentration over densely populated regions was simulated to increase in 2050 in comparison with that in 2000 for both the SRES A2 and B1 scenarios. The sulfate concentration and sulfur wet deposition were predicted to decrease over Europe and North America, whereas to increase around East Asia. Tegen et al. (2000) suggested that the optical thickness of sulfate aerosols has been increased rapidly in the past few decades in Asia. The simulated results also indicated that heavily emitted anthropogenic pollutants from the East Asian continent will affect the radiative and chemical conditions seriously not only within the continent but also around Japan and the North Pacific due to long-range transport in the next few decades. It is therefore important to monitor the environmental condition in these areas and to invest in the technology for reducing emissions of sulfuric, nitric, and carbonaceous pollutants in developing countries of Asia.

The BC mass ratio to the sulfate aerosols is predicted to become large gradually in the future in the simulation along the SRES scenarios, so that the aerosol single scattering albedo is calculated to become smaller in 2050 than in 2000 at the mid- and high-latitudes of the Northern Hemisphere. The IPCC (1996) concluded that the positive radiative forcing by greenhouse gases from 2000 to 2100 is offset with a temporal increase of the SO_2 emission along the IS92a scenario more than with

the scenario of the constant emission of the year 1990 because of the cooling effect of sulfate aerosols. The IS92a scenario, however, predicted much larger anthropogenic SO_2 emission than that of the newest IPCC scenario, i.e., the SRES scenarios. It is generally said that aerosol particles cool the earth's atmosphere by the direct effect, but the simulated future small single scattering albedo suggests that this cooling effect may be reduced substantially if the BC contribution continues to rise in the future. Moreover, it is possible to accelerate the global warming due to the aerosol direct effect if the future BC emission surpasses the estimate of the SRES scenarios. East Asia does not have many observation sites for aerosol radiative properties, and then it is expected that many useful understandings on aerosol concentrations, compositions, and optical properties are obtained through the intensive observation campaign such as the Asian Pacific Regional Aerosol Characterization Experiment (ACE–Asia).

Acknowledgments

We thank the GCM group of CCSR and NIES for supporting our work, especially Dr. A. Numaguti of the Hokkaido University who is a main developer of the CCSR/NIES AGCM, and we regret his death in a sudden accident. We are also grateful to Prof. T. Takamura of the Center for Environmental Remote Sensing (CEReS), Chiba University who kindly allowed us to use the SKYNET site data set of the sky radiometer. Thanks are extended to Drs. H. Nagata and T. Watanabe of the Japan Sea National Fisheries Research Institute, Dr. N. Sugimoto of the National Institute for Environmental studies, and Dr. M. Shiobara of the National Institute of Polar Research for maintenance of continual observations.

References

Benkovitz, C.M., M.T. Scholtz, J. Pacyna, L. Tarrasón, J. Dignon, E.C. Voldner, P.A. Spiro, J.A. Logan and T.E. Graedel, 1996: Global gridded inventories of anthropogenic emissions of sulfur and nitrogen. *J. Geophys. Res.*, **101**, 29239–29253.

Brossset, C. and A. Akerstrom, 1972: Long distance transport of air pollutants—Measurements of black air-borne particulate matter (soot) and particle-borne sulphur in Sweden during the period of September–December 1969. *Atmos. Environ.*, **6**, 661–673.

Collins, W.J., D.S. Stevenson, C.E. Johnson and R.G. Derwent, 1997: Tropospheric ozone in a global-scale three-dimensional Lagrangian model and its resonse to NO_x emission controls. *J. Atmos. Chem.*, **26**, 223–274.

Cooke, W.F. and J.J.N. Wilson, 1996: A global black carbon aerosol model. *J. Geophys. Res.*, **101**, 19395–19409.

Dubovik, O. and M.D. King, 2000: A flexible inversion algorithm for retrieval of aerosol optical properties from Sun and sky radiance measurements. *J. Geophys. Res.*, **105**, 20673–20696.

Feichter, J., U. Lohmann and I. Schult, 1997: The atomospheric sulfur cycle in ECHAM–4 and its impact on the shortwave radiation. *Clim. Dyn.*, **13**, 235–246.

Higurashi, A., T. Nakajima, B.N. Holben, A. Smirnov, R. Frouin and B. Chatenet, 2000: A study of global aerosol optical climatology with two channel AVHRR remote sensing. *J. Climate*, **13**, 2011–2027.

Hobbs, P.V., J.S. Reid, R.A. Kotchenruther, R.J. Ferek and R. Weiss, 1997: Direct radiative forcing by smoke from biomass burning. *Science*, **275**, 1776–1778.

Holben, B.N., T.F. Eck, I. Slutsker, D. Tanré, J.P. Buis, A. Setzer, E. Vermote, J.A. Reagan, Y.J. Kaufman, T. Nakajima, F. Lavenu, I. Jankowiak and A. Smirnov, 1998: AERONET—A federated instument network and data archive for aerosol characterization. *Remote Sens. Environ.*, **66**, 1–16.

———, D. Tanré, A. Smirnov, T.F. Eck, I. Slutsker, N. Abuhassan, W.W. Newcomb, J.S. Schafer, B. Chatenet, F. Lavenu, Y.J. Kaufman, J. Vande Castle, A. Setzer, B. Markham, D. Clark, R. Frouin, R. Halthore, A. Karnieli, N.T. O'Neill, C. Pietras, R.T. Pinker, K. Voss and G. Zibordi, 2001: An emerging ground-based aerosol climatology: Aerosol optical depth from AERONET. *J. Geophys. Res.*, **106**, 12067–12097.

IPCC (The Intergovernmental Panel on Climate Change), 1992: *Climate Change 1992: The Supplementary Report to the IPCC Scientific Assessment.* J.T. Houghton, B.A. Callander and S.K. Varney, Eds., Cambridge Univ. Press, 200 pp.

———, 1996: *Climate Change 1995: The Science of Climate Change.* J.T. Houghton, L.G. Meira Filho, B.A. Callander, N. Harris, A. Kattenberg and K. Maskell, Eds., Cambridge Univ. Press, 572 pp.

———, 2000: *Special Reports on Emissions Scenarios.* N. Nakicenovic and R. Swart, Eds., Cambridge Univ. Press, 612 pp.

———, 2001: *Climate Change 2001: The Scientific Basis.* J.T. Houghton, Y. Ding, D.J. Griggs, M. Noguer, P.J. van der Linden, D. Xiaosu, K. Maskell and C.A. Johnson, Eds., Cambridge Univ.

Press, 896 pp.

Kato, N. and H. Akimoto, 1992: Authropogenic emissions of SO_2 and NO_x in Asia: Emission inventories. *Atmos. Environ.*, **26A**, 2997–3017.

Kiehl, J.T., T.L. Schneider, P.J. Rasch, M.C. Barth and J. Wong, 2000: Radiative forcing due to sulfate aerosols from simulations with the National Center for Atomospheric Research Community Climate Model. Version 3, *J. Geophys. Res.*, **105**, 1441–1457.

Langner, J. and H. Rodhe, 1991: A global three-dimensional model of the tropospheric sulfur cycle. *J. Atmos. Chem.*, **13**, 225–263.

Lefohn, A.S., J.D. Husar and R.B. Husar, 1999: Estimating historical anthropogenic global sulfur emission patterns for the period 1850–1990. *Atmos. Environ.*, **33**, 3435–3444.

Numaguti, A., M. Takahashi, T. Nakajima and A. Sumi, 1995: Development of an atmospheric general circulation model. *Climate System Dynamics and Modeling*, T. Matsuno, Ed., Center for Climate System Research, University of Tokyo, 1–27.

Nakajima, T., M. Tsukamoto, Y. Tsushima, A. Numaguti and T. Kimura, 2000: Modeling of the radiative process in an atomospheric general circulation model. *Appl. Opt.*, **39**, 4869–4878.

Nozawa, T., S. Emori, A. Numaguti, Y. Tsushima, T. Takemura, T. Nakajima, A. Abe-Ouchi and M. Kimoto, 2001: Projections of future climate change in the 21st century simulated by the CCSR/NIES CGCM under the IPCC SRES scenarios. *Present and Future of Modeling Global Environmental Change toward Integrated Modeling*, T. Matsuno and H. Kida, Eds., Terra Scientific Publishing, 15–28.

Penner, J.E., C.C. Chuang and K. Grant, 1998: Climate forcing by carbonaceous sulfate aerosols. *Clim. Dyn.*, **14**, 839–851.

Sudo, K. and M. Takahashi, 2001: Simulation of tropospheric ozone changes during 1997–1998 El Niño: Meteorological impact on tropospheric photochemistry. *Geophys. Res. Lett.*, **28**, 4091–4094.

Takemura, T., H. Okamoto, Y. Maruyama, A. Numaguti, A. Higurashi and T. Nakajima, 2000: Global three-dimensional simulation of aerosol optical thickness distribution of various origins. *J. Geophys. Res.*, **105**, 17853–17873.

———, T. Nakajima, O. Dubovik, B.N. Holben and S. Kinne, 2001: Single scattering albedo and radiative forcing of various aerosol species with a global three-dimensional model. *J. Climate*, in press.

Tegen, I., D. Koch, A.A. Lacis and M. Sato, 2000: Trends in tropospheric aerosol loads and corresponding impact on direct radiative forcing between 1950 and 1990: A model study. *J. Geophys. Res.*, **105**, 26971–26989.